Journal of Computer Assisted Tomography
9(2):252–257, March/April

Edge Artifacts in MR Images: Chemical Shift Effect

Evelyn E. Babcock, Libby Brateman, Jeffrey C. Weinreb, Sherye D. Horner, and Ray L. Nunnally

Abstract: The boundaries of some organs as seen in clinical magnetic resonance images appear to be asymmetric. This effect is caused by chemical shift differences between the resonant frequencies of the hydrogen nuclei of water and fat. The zeugmatographic technique maps resonant frequencies to unique spatial locations. These differences in resonant frequencies can appear as artifactual misplacement of information as this one-to-one correspondence is lost. Various phantoms are used to demonstrate that the boundary artifact appears only in the direction of the read (frequency-encoding) gradient when media of two different chemical shifts are separated by an interface. When the relative shift is less than the width of the interface, the boundary appears to be asymmetric; when the relative shift is greater than the width of the interface, a bright band is seen along one edge with a dark band along the other. This artifact is more pronounced in low resolution images than in high resolution images, and these effects are seen even when the relative chemical shift is smaller than a pixel bandwidth. These effects are explained both conceptually and analytically. The clinician should be aware of the potential presence of this artifact at boundary interfaces that bear diagnostic significance. **Index Terms:** Chemical shift imaging—Nuclear magnetic resonance, artifacts—Nuclear magnetic resonance.

Careful observation of clinical magnetic resonance (MR) images indicates an asymmetry in the boundaries of some organs. Figure 1 demonstrates this effect bordering the kidneys and could possibly be misinterpreted as a thickened renal capsule. A dark border appears on the right edge of each kidney in the transaxial orientation (Fig. 1a). In the coronal orientation (Fig. 1b) the dark border is on the inferior edge of each kidney. Although a similar finding has been termed a "linear edge" artifact (1), it is demonstrated here that this asymmetry is due to chemical shift differences. These boundary artifacts appear clinically where predominantly water-filled compartments abut fatty deposits. The compartmentation allows the chemical shift differences between the hydrogen nuclei of water and the mobile lipid protons of adjacent fat to distort spatial information that is translated into a displacement artifact in the image. In addition to the kidney some of the other organs surrounded by fat that have demonstrated chemical shift artifacts are the spleen, heart, and breast. The artifact is also present at the intervertebral disk boundary.

From the Department of Radiology, University of Texas Health Science Center at Dallas, 5323 Harry Hines Boulevard, Dallas, TX 75235, U.S.A. Address correspondence and reprint requests to Dr. E. E. Babcock.

MATERIALS AND METHODS

A Diasonics MT/S imaging system operating at 0.35 T was used in this study. Images were obtained using a two-dimensional Fourier transform (2DFT) technique and a spin-echo pulse sequence (2). Personal communications with the manufacturer (Diasonics NMR, Inc., South San Francisco, CA) indicate that the bandwidth or frequency resolution of a pixel is approximately 110 Hz independent of the image spatial resolution. Furthermore, the "read" or "frequency-encoding" gradient amplitudes range from approximately 0.1 to 0.3 G/cm for the lowest to highest spatial resolution images, respectively. The chemical shift difference between fat and water, if assumed to be 3.5 parts per million (ppm), is 52.5 Hz at 0.35 T. Thus, this frequency

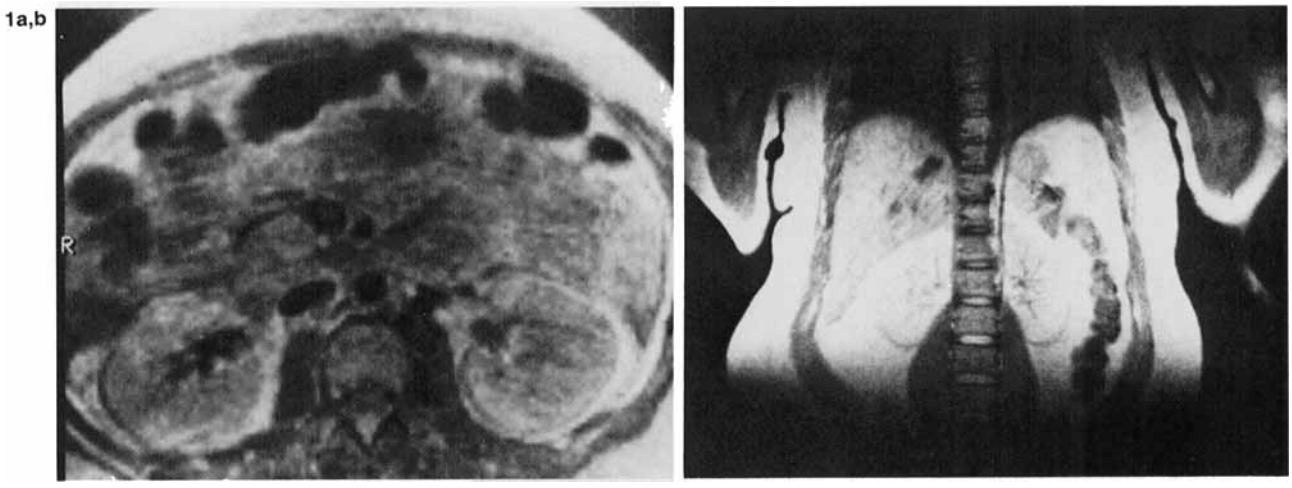

FIG. 1. An apparently asymmetric renal capsule is seen bordering both kidneys **(a)** as a dark border on the right edge in a transaxial orientation, and **(b)** as a dark border on the inferior edge in a coronal orientation.

difference of 53 Hz is slightly less than one-half the bandwidth of a display pixel (48%).

Phantom Studies

To model a kidney and its surrounding fat the phantom initially studied was a water-filled balloon in a beaker of mineral oil. This phantom was imaged in the transaxial, sagittal, and coronal orientations with echoes at 28 and 56 ms (Fig. 2). The artifact, a dark border along one interface and a bright border on the opposite interface, consistently appeared in the direction of the read gradient.

The second phantom studied consisted of several 20 mm NMR tubes containing a variety of liquids in either a water or an oil bath. The use of NMR tubes guaranteed a uniform wall thickness of approximately 1 mm. The various chemicals studied are listed in Table 1, along with their chemical shifts in ppm relative to tetramethylsilane and their volumetric magnetic susceptibilities. The frequency difference in hertz at the field strength used in this study for two compounds may be obtained by subtracting the relevant chemical shifts in hertz given in Table 1. Table 1 also demonstrates that the compounds used in this phantom differ in magnetic susceptibility as well as chemical shift. The results indicate that both substantial differences in chemical shift and large variations in magnetic susceptibility (which affect the proton precession frequency) create frequency shifts sufficiently large to cause asymmetric boundaries. Comparison of the phantom in water (Fig. 3a) with the phantom in oil (Fig. 3b) emphasizes the effect of the chemical shift differences. For example, Tube 3 contains benzene, which has a chemical shift difference from oil of approximately 75 Hz and from water of approximately 40 Hz. As expected, the asymmetry of the benzene tube is more pronounced in the oil phantom (Fig. 3b) than in the water phantom (Fig. 3a). Furthermore, Tube 7 contains isopropanol, which has essentially the same chemical shift as oil; therefore, no shift is seen in Fig. 3b. However, isopropanol is chemically shifted from water, and the effect of this chemical shift difference is observed in Tube 7 of the water phantom (Fig. 3a). In addi-

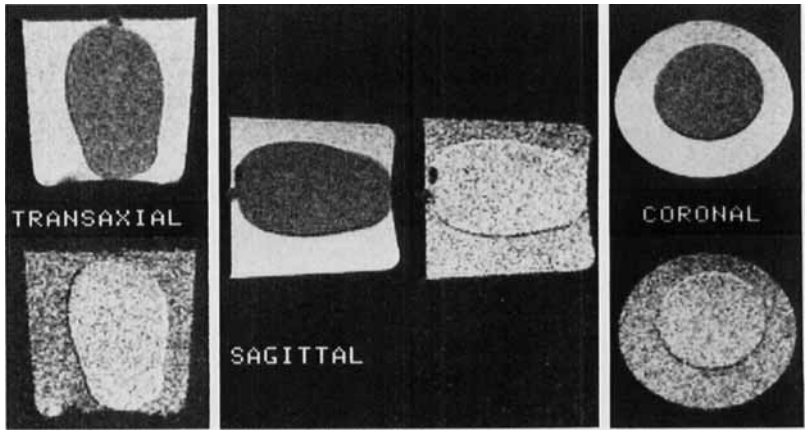

FIG. 2. First and second echo (28 and 56 ms, respectively) images of a water-filled balloon in a beaker of mineral oil show dark and bright boundary artifacts in the direction of the read gradient in three orientations. **(left):** Transaxial (top, first echo; bottom, second echo); **(middle):** sagittal (left, first echo; right, second echo); and **(right):** coronal (top, first echo; bottom, second echo).

TABLE 1. *Chemical shifts and magnetic susceptibilities of compounds imaged*

Tube number[a]	Compound	Chemical shift[b] (ppm)	(Hz at 15 MHz)	Magnetic susceptibility (5) ($\times 10^{-6}$ cm^{-3})
1	Water	4.5	67.5	−0.7
2	Mineral oil	2.0	30.0	*c*
3	Benzene	7.2	108	−0.6
4	Colbalt chloride (0.1 *M*)	*c*	*c*	+126
5	Magnesium sulfate (1 *M*)	*c*	*c*	−34
6	Acetone	2.2	33.0	−0.5
7	Isopropanol CH_3	1.1	16.5	−0.6
	CH	3.2	48.0	
	OH	3.9	58.5	
8	Sodium fluoride (0.9 *M*)	4.5	67.5	−1.3
9	Ethanol CH_3	1.1	16.5	−0.6
	CH_2	3.5	52.5	
	OH	4.3	64.5	
10	Chloroform	7.3	110	−0.7

[a] Tube numbered according to Fig. 3.
[b] Referenced to tetramethysilane (6).
[c] Exact value unknown.

tion, since isopropanol and benzene are each chemically shifted from water by approximately 40 Hz, but in opposite directions, the asymmetry of the NMR tube walls containing these compounds is discernible in opposing directions (Tubes 3 and 7 of Fig. 3a).

Studies were conducted on a third phantom that consisted of several NMR tubes of various diameters placed concentrically. A 5 mm NMR tube containing benzene was placed within a 12 mm tube of acetone. The two tubes were then placed in the center of a 20 mm NMR tube containing benzene, which was situated in a beaker of acetone. Thus, this phantom provided alternating benzene-acetone interfaces. These two compounds were chosen, not because of their physiological significance, but because they possess essentially identical magnetic susceptibilities, and each has a single proton resonance, differing in chemical shift from each other by approximately 5 ppm (75 Hz at 0.35 T). Figure 4 shows images of the phantom obtained with 1.7 and 0.8 mm pixel dimensions (low resolution and high resolution, respectively). The asymmetry of the NMR tubes is striking and is more pronounced in the lower resolution image (Fig. 4a).

DISCUSSION

One of the fundamental principles in MR imaging is the ability to encode spatial information into both

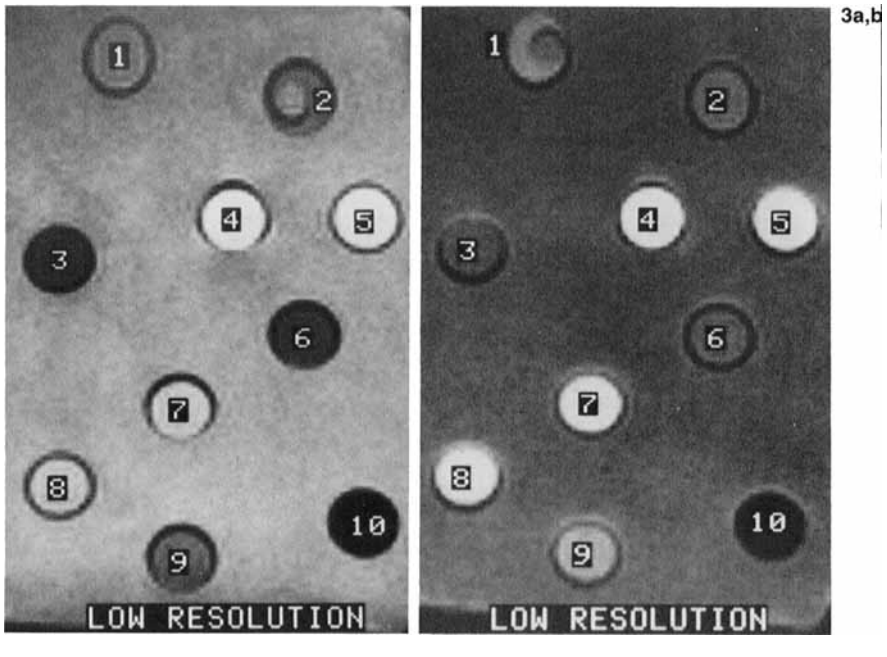

FIG. 3. Images of 20 mm MR tubes containing various compounds (described in Table 1) surrounded by a bath of **(a)** water and **(b)** oil. The wall thickness of the tubes is approximately 1 mm. In (a) Tube 2 contains a smaller tube of water, and in (b) Tube 1 contains a smaller tube of oil. Apparent asymmetries in the tube walls are noted with differences between (a) and (b). (See text for further discussion.)

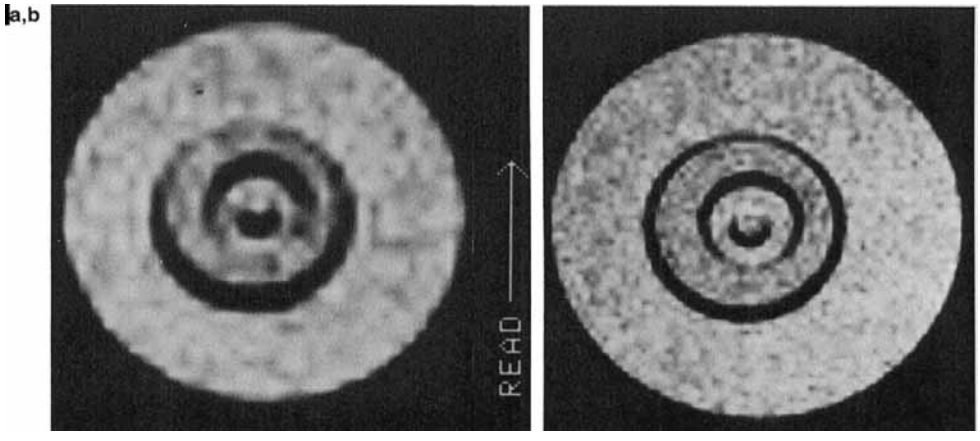

FIG. 4. Alternating interfaces of acetone and benzene (acetone is the outermost medium) demonstrate chemical shift asymmetries in both **(a)** low and **(b)** high resolution images. This effect is seen to be greater in (a).

the frequency and phase components of an MR signal. When an isotope possessing a magnetic moment is placed in a static magnetic field B_0, it precesses about this magnetic field. The angular frequency of precession ω_0 is defined by the Larmor equation as $\omega_0 = \gamma B_0$, where γ is the gyromagnetic ratio, a constant for a given nuclide. However, innate differences in magnetic shielding due to the variations in the chemical environments of nuclei cause a nucleus to experience an "effective" magnetic field strength B_{eff}, which differs from B_0, thereby changing the Larmor equation to $\omega = \gamma B_{\text{eff}}$. Such magnetic shielding results in variations in the Larmor frequency known as chemical shifts.

Since the frequency of precession is proportional to the magnetic field, the application of a magnetic field gradient causes the precession frequency of a nucleus to be a linear function of its position with respect to the gradient. Specifically, the precession frequency is

$$\omega_x = \gamma(B_0 - xG_x),$$

where x is the spatial location, and G_x represents a linear magnetic field gradient in the x-direction. Since the 2DFT imaging technique translates the frequency information obtained in the read direction directly into spatial information, this technique is unable to discriminate between frequency shifts due to chemical shift differences and those due to the valid encoding of true differences in position by the read gradient. Therefore, a relative "displacement" of the chemically shifted species in the direction of the read gradient may be apparent in the final image.

The equations defining the frequencies of nuclei A and B at specific locations x_A and x_B along the gradient are:

$$\omega_A = \omega_{0A} + x_A\gamma G_x$$

and

$$\omega_B = \omega_{0B} + x_B\gamma G_x$$

where G_x is the read gradient. The precession frequency ω_A is a sum of the innate frequency of the nucleus derived from the chemical shift ω_{0A} and the frequency resulting from the spatial location of the nucleus along the read gradient $x_A\gamma G_x$. If nuclei A and B are chemically shifted from each other, i.e., ω_{0A} is not equal to ω_{0B}, a frequency difference results in addition to that due to the spatial positions of the nuclei. Since this imaging technique translates frequency information obtained in the read direction directly into spatial information, a misplacement in the spatial mapping results. This effect is represented pictorially in Fig. 5 in which compound A is bordered on both sides by compound B. Figure 5a depicts the image obtained when compounds A and B have the same chemical shift, and Fig. 5b represents the image obtained when there is a chemical shift difference between compounds A and B. It is seen that the shift of spatial information causes a signal enhancement on the side for which signals from A and B overlap and a concomitant

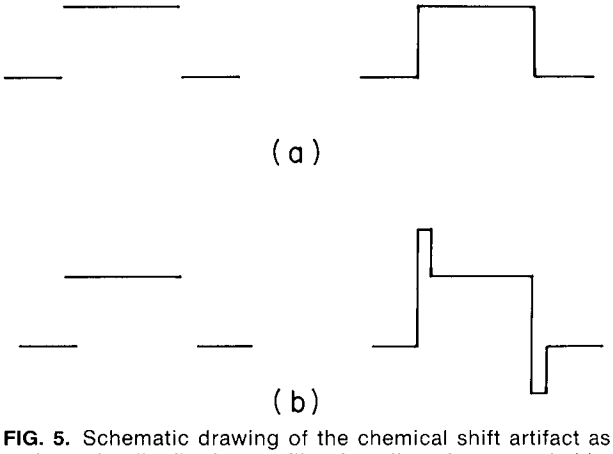

FIG. 5. Schematic drawing of the chemical shift artifact as an intensity distribution profile of medium A surrounded by medium B. In **(a)** there is no relative chemical shift at the interface between media A and B, and there is no boundary artifact in the composite. In **(b)** the chemical shift of B with respect to A causes misplacement of information from medium B (i.e., a shift to the right) and, consequently, boundary artifacts appear in the composite.

decrease in signal on the opposite side. The final image can thus be thought of as a composite, a summation of spatial information regarding fat intensity (the "fat" image) and water intensity (the "water" image), in which these two images are displaced from one another along the dimension of the read gradient by the chemical shift difference between fat and water. Recent works demonstrating a method of separation of a composite clinical image into "fat" and "water" images have shown boundary artifacts at the interfaces (3,4).

As may be observed from the artifact in the phantom studies, the dark band is always detectable, but the enhanced or bright band is not consistently observed. This bright band, present when there is an overlapping of the signals from the chemically shifted regions (Fig. 5b), is demonstrated in the kidney phantom (Fig. 2) in which a definite band of increased intensity (the enhanced boundary) is observed. However, no overlap of the chemically shifted regions is observed in the second phantom (Fig. 3). The determining factors of whether an enhanced boundary is present are (a) the chemical shift difference, (b) the thickness of the interface that separates the chemically shifted species, and (c) the amplitude of the gradient used to acquire the data. In Fig. 2b (2.0 mm pixel dimensions) the read gradient amplitude is approximately 53 Hz/mm. If the interface is assumed to be 0.1 mm thick, the oil and water compartments are separated by fewer than 6 Hz. Since the chemical shift difference between mineral oil and water is roughly 38 Hz, their frequency difference is greater than the interface thickness. Thus, in the image the two regions overlap, yielding an enhanced boundary. For the 1.7 mm spatial resolution protocol used to obtain the images of the second phantom studied (Fig. 3), the gradient amplitude is approximately 66 Hz/mm. The NMR tube walls, which are 1 mm thick, yield a separation of approximately 66 Hz between the various liquids. Any intensity enhancement is therefore possible only for a chemical shift difference greater than 66 Hz.

This frequency-encoding of the physical interface is the basis for the artifact being more pronounced in lower resolution than higher resolution images (Fig. 4). The reader is reminded that the frequency resolution of a display pixel is 110 Hz regardless of the gradient strength used. The frequency spread due to chemical shift is a constant fraction of the total frequency spread of a display pixel in both high and low resolution images because the chemical shift frequency difference is inherent and is not due to physical location. The lower resolution images (1.7 mm pixel dimensions) are produced with a smaller read gradient amplitude (66 Hz/mm) than those of higher resolution (0.8 mm pixel dimensions with 133 Hz/mm). Hence, the chemical shift frequency difference represents a larger spatial spread in the low resolution image and is therefore more pronounced.

Even when the distortion of spatial information and resulting displacement due to chemical shift differences is small compared with the bandwidth per pixel, the effect is definitely apparent in the image. Figure 6 shows images resulting from a computer simulation of the chemical shift. The upper half of each image shows the resultant pixel densities when media on either side of the boundary have the same chemical shift. The lower half of each image shows the resultant pixel densities when the outside medium is shifted to the right with respect to the inner medium and interface. In Fig. 6 the chemical shift difference simulated corresponds to that of the clinical images (48% of a pixel width). In Fig. 6a this shift is less than the interface or boundary width (1.25 pixels). In this case the boundary seems to be asymmetric since the shift of the outside medium causes the left border to appear narrower and the right border wider. When the shift is greater than the boundary thickness, signals from the inner and outer regions overlap, yielding an enhanced or bright boundary on the left side with a dark border on the right side. This situation is simulated in Fig. 6 in which the boundary is a width of 0.25 pixel.

Thus, Fig. 6 demonstrates that a chemical shift difference considerably less than the width of a display pixel is sufficient to produce an image artifact. This asymmetric artifact occurs in a plane (i.e., of zero thickness) as has been demonstrated with the images shown in Fig. 6 simulating the chemical shift at fat–water interfaces. Application of slice-selection gradients might also produce chemical shift artifacts perpendicular to the slices, which would yield nonplanar slices and artifactual displacements into or out of the plane of section.

It is tempting to increase the gradient strength in an effort to eliminate the chemical shift artifact. The increased gradient strength causes the physical boundary to be represented by an increased frequency spread while the chemical shift is not affected, and the chemical shift displacement thus becomes insignificant when compared with the physical boundary. However, the cost of implementing this particular solution might be too great in terms of the signal-to-noise ratio, since more noise will be introduced without a concomitant increase in signal strength.

In conclusion, this article demonstrates that chemical shift differences can result in image artifacts observable in the direction of the read or frequency-encoding gradient. Depending on the relative chemical shift between the media on either side of an interface, the thickness of the interface, and the gradient strength, the artifact may appear as two asymmetric borders or one dark and one enhanced boundary. That this effect is seen for chemical shift differences corresponding to a fraction of a pixel

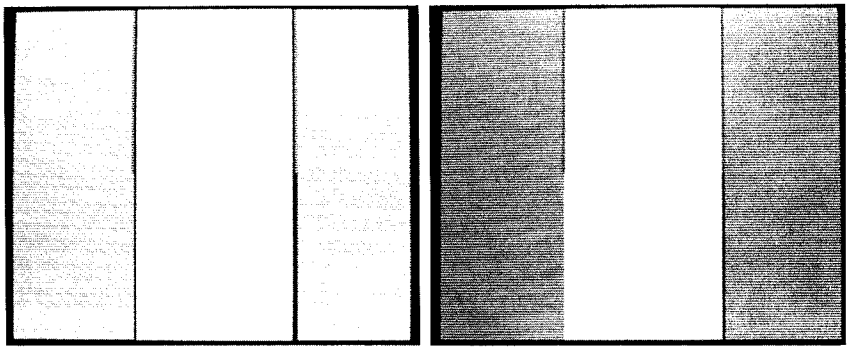

FIG. 6. A computer simulation of the chemical shift artifact. The upper half of each image shows no relative shift with respect to the two media; the lower half demonstrates the same boundary with a shift corresponding to 0.48 pixel width. The boundary widths are **(a)** 1.25 and **(b)** 0.25 pixel. When the shift is smaller than the boundary width as in (a), the dark interface appears asymmetric; when the shift is greater as in (b), there is an artifactual bright boundary at one side and a dark boundary at the opposite side.

has been demonstrated by computer simulation; this shift can be thought of as a "partial-volume" effect in the plane of the pixel in the read gradient direction. Even though a boundary is smaller than a pixel dimension, it is seen in the image because the pixel has a different average signal intensity from its surroundings. For the same reason, shifted data, even though the shift is less than a pixel, can also result in an average pixel value different from the surrounding media, and, therefore, detectable in the image. It is such a shift, resulting from the chemical shift difference between fat and water, that causes the enhanced boundary artifact seen in some clinical images.

The clinical significance of recognizing and understanding the origin of this artifact lies in not mistaking it for real anatomic structure. As demonstrated in Fig. 1, this artifact can be recognized by its characteristic appearance as a thin, low-intensity line perpendicular to the direction of the frequency-encoding gradient. Confinement within or extension beyond this thin, low-intensity line cannot be used as a criterion for staging neoplasms or disease processes.

Acknowledgment: This work was supported in part by grants from the National Institutes of Health, number 5R01 HL27472-03 (RLN); Public Health Service, number 5T32 HL07362 (EEB); and Diasonics NMR, Inc. The authors wish to acknowledge the excellent technical assistance of Judy Behrens, Frank Gorishek, and Cindy Miller.

REFERENCES

1. Hricak H, Williams RD, Moon KL, et al. Nuclear magnetic resonance imaging of the kidney: renal masses. *Radiology* 1983;147:765–72.
2. Crooks LE, Hoenninger J, Arakawa M, et al. High-resolution magnetic resonance imaging: technical concepts and their implementation. *Radiology* 1984;150:163–71.
3. Dixon WT, Faul DD. Proton spectroscopic imaging at 0.35 T [Abstract]. In: *Proceedings of Society of Magnetic Resonance in Medicine*. Berkeley, CA: Society of Magnetic Resonance in Medicine, 1984:193.
4. Rosen BR. The applications of proton chemical shift imaging [Abstract]. In: *Proceedings of Society of Magnetic Resonance in Medicine*. Berkeley, CA: Society of Magnetic Resonance in Medicine, 1984:636.
5. Weast RC, ed. *Handbook of chemistry and physics*, 55th ed. Cleveland: CRC Press, 1974.
6. Pouchert CJ, ed. *Aldrich library of NMR spectra*, 2nd ed. Milwaukee: Aldrich Chemical Co., 1983.